Structure of DNA toroids and electrostatic attraction of DNA duplexes

2005 J. Phys.: Condens. Matter 17 1363

(http://iopscience.iop.org/0953-8984/17/8/015)

INSTITUTE OF PHYSICS PUBLISHING JOURNAL OF PHYSICS: CONDENSED MATTER

J. Phys.: Condens. Matter **17** (2005) 1363–1374 doi:10.1088/0953-8984/17/8/015

Structure of DNA toroids and electrostatic attraction of DNA duplexes

A G Cherstvy

Institut für Festkörperforschung, Forschungszentrum Jülich, D-52425 Jülich, Germany

Received 4 November 2004, in final form 18 January 2005
Published 11 February 2005
Online at stacks.iop.org/JPhysCM/17/1363

Abstract

DNA–DNA electrostatic attraction is considered as the driving force for the formation of DNA toroids in the presence of DNA condensing cations. This attraction comes from the DNA helical charge distribution and favours hexagonal toroidal cross-sections. The latter is in agreement with recent cryo-electron microscopy studies on DNA condensed with cobalt hexammine. We treat the DNA–DNA interactions within the modern theory of electrostatic interaction between helical macromolecules. The size and thickness of the toroids is calculated within a simple model; other models of stability of DNA toroids are discussed and compared.

1. Introduction

1.1. DNA toroidal condensation

In vivo, DNA is condensed to fit a small volume accessible for it and to ensure protection of genetic material. DNA condensation occurs in chromosomes [1–3], in some bacteria [4, 5], and in bacteriophage heads [6, 7]. In some phages, DNA can adopt a toroidal-like structure [8, 9]. Within sperm cell nuclei of many vertebrates the DNA is also packaged into toroids by small basic proteins (protamines) [10, 11]. *In vitro*, toroidal DNA condensation is induced by various condensing agents [12–22]. The size and shape of DNA toroids is only slightly dependent on DNA molecular weight: typically, the toroid outer radius is ∼500 Å and the inner radius is ∼150 Å (for DNA length from 400 base pairs (bp) to 40 kbp) [18]; see figure 1(A). The distribution of toroidal dimensions can be quite broad but usually the outer and inner radii are correlated [22]. Toroids may consist of one or several DNA [20]; a single DNA can also comprise many toroids (like mammalian sperm DNA [10]). In toroids DNA adopts the canonical B-form [20].

DNA is condensed by tri- and higher-valent mobile cations (cobalt hexammine (cohex) [18, 9], spermidine [12, 21, 22], spermine [18]) and by some charged proteins (polylysine [13, 23], protamine [10], H1 histone proteins [24]). Some viruses also use spermidine for compaction their DNA; spermidine is also present in the cell nucleus, being

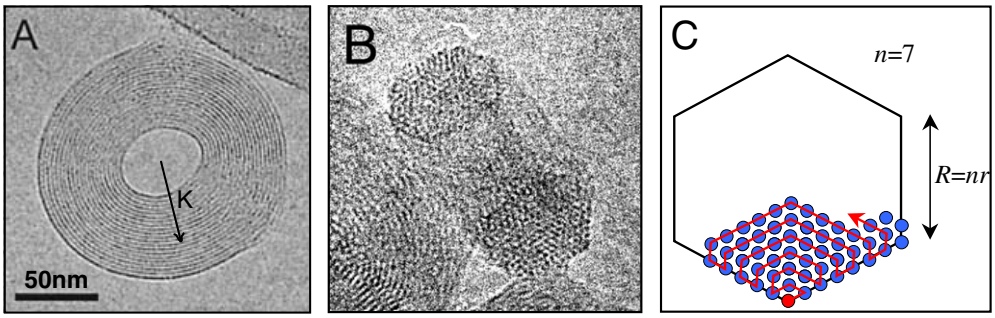

Figure 1. Fine structure of DNA toroids detected by cryoelectron microscopy [48] in 20 μg ml^{-1} solution of λ-phage DNA in 0.2 mM solution of $Co(NH_3)_6Cl_3$ (A: top view, B: side view) and the schema of the hexagonal toroidal cross-section with one of the possible DNA wrapping paths in toroids (C). Pictures A and B are taken from [48], with permission of N Hud.

(This figure is in colour only in the electronic version)

involved in regulation of the cell activity. Usually, the addition of a simple salt in solution requires higher concentrations of multivalent cations to provoke DNA condensation [18, 19]. Toroidal condensates can resolubilize upon the addition of NaCl; at elevated temperatures DNA condensation requires a smaller amount of cohex [14].

Cohex is five times more efficient for DNA condensation than spermidine^{3+} [14, 18] although both are trivalent. There is a tendency that cations that bind into the *major* DNA groove are more efficient in DNA condensation. Some transition metal cations like Mn^{2+} also condense DNA [5]. This is not surprising because under the osmotic stress the Mn-DNAs reveal an attraction at surface-to-surface separation of ∼10 Å [25, 26]. DNA supercoiling and elevated temperatures favour condensation [27]. In alcohol–water mixtures, $MgCl_2$ can also induce condensation [16]: alcohols are typically excluded from the DNA phase, exerting an osmotic stress on it and forcing DNA together [28, 29]. In some cases, the aggregation of toroids into higher-order structures can occur [20, 30].

Depending on the solvent conditions and DNA stiffness, toroidal and rod-like [18, 23] as well as sphere-like [31] DNA condensates appear (rods can coexist with and convert into toroids [18, 31]). In poor solvent, either spherical globules or toroids are formed, minimizing the contact area of condensate with the solvent and optimizing the DNA bending energy. DNA can be condensed into toroids also on surfaces, with no mobile condensing agents in solution [32]. Naturally, the dimensions of DNA toroids depend on the strength of DNA–DNA interaction and DNA bending flexibility l_p [33, 34]. Smaller toroids are formed of DNA with intrinsically bendable AT-rich tracks (that allows control of the toroidal dimensions [35, 36] making toroids attractive tools for gene therapy purposes [37]).

1.2. The nature of DNA–DNA attraction and its specificity

B-DNA is a highly charged molecule (one elementary charge per 1.7 Å along the axis). In solution, cations adsorb on the DNA, but where and how strongly do they bind are still matters of debate. Many multivalent cations bind (specifically) in the major DNA groove, Ca^{2+} and Mg^{2+} are likely to bind electrostatically on DNA phosphate strands or in the minor groove, Mn^{2+} and Cd^{2+} can bind in both DNA grooves. Some divalent cations (Mn^{2+}, Cd^{2+}) cause DNA condensation [25] whereas others (Ca^{2+}, Mg^{2+}) do not [18].

It is established that DNA condenses when about 90% of its charge is neutralized [16, 18]. However, the mechanisms and forces triggering the DNA collapse are not exactly known. This might be the hydration forces between highly hydrated DNA (about 20 waters/bp for B-DNA) [38] or the electrostatic attraction between the duplexes [39–42]. Correlation of fluctuations of condensed counterions can also cause attraction between likely uniformly charged rods, as was first predicted by Oosawa [43] and developed in a number of theoretical works [44][1,2] and computer simulations [45, 46]. Such an attraction mechanism however is not cation-specific. We show below that the *DNA helical structure* and the positions of adsorbed cations are important for the description of DNA condensation.

The electrostatic interaction energy between two double *spirals of charges* has been calculated recently by Kornyshev and Leikin as the exact solution of the Poisson–Boltzmann equation [39]. The attraction was shown to appear naturally between two DNA duplexes with the spine of adsorbed cations in the grooves [40], with no invocation to counterion fluctuations. In this theory, the DNA helical charge distribution is the reason for the DNA–DNA attraction. Namely, the 'electrostatic zipper' formed by the phosphates of one DNA and the cations adsorbed in the grooves of another DNA [40] ensures the charge alternation along the DNA contact and causes the attraction. This theory and its modifications have been used to describe several puzzling experimental observations: the decay lengths in interaction of many biological helices (collagen, DNA, guanosine, etc); the overwinding of DNA from 10.5 bp/turn in solution to 10.0 bp/turn in dense assemblies [47]; the zipper motif for DNA condensation [40]; the mechanism for electrostatic recognition of DNA duplexes from a distance [41, 42]; DNA azimuthal frustrations on the hexagonal lattice [42], etc.

1.3. Structure and stability of DNA toroids

In toroids, DNA prefers to pack in a hexagonal lattice with DNA–DNA separation of $r \approx 28$ Å [18, 48] (see also [6, 7, 49]). At $r = 28$ Å, DNA–DNA attraction has been detected in osmotic stress experiments on hexagonal DNA assemblies in the presence of Mn and cohex [25, 50]; the Kornyshev–Leikin theory [39] also predicts attraction at such r. Recent cryo-electron microscopy studies have shown [48] that cross-sections of DNA toroids are often nearly hexagonal, figure 1(B), and consist of *closed shells* of packed DNA (different kinds of cross-sections are possible as well [22, 48]). Hexagonal cross-sections maximize the number of attractive DNA–DNA contacts: 'inner' DNA with six nearest neighbours bring more attraction than 'outer' DNA do, with three or four neighbours.

Several models for toroidal collapse of charged semiflexible (DNA-like) polymer have been suggested [18, 31, 51–53]. The collapse was considered as a polymer-induced condensation [31, 51, 53] or as a result of attractive hydration forces between DNA [18] or as a result of correlated fluctuations of condensed cations. The direct electrostatic attraction between the *spirals* of DNA charges [39, 42] however has not been considered before as the source of formation of DNA toroids. We do it in the present paper.

[1] This type of DNA–DNA attraction also requires an alternation of positive and negative charges on molecular surfaces. The DNA is modelled in these theories as a uniformly charged rod and adsorbed cations can adjust their positions upon approach of DNAs. The latter is however hardly justified especially for trivalent ions since their irreversible adsorption on the DNA can occur. The position and affinity of cations to adsorption sites are imposed by the DNA helical structure. This determines the period of charge alternation along DNA and influences the intermolecular forces.

[2] DNA–DNA attraction may also come from a *bridging/cross-linking* of nearest helices by chain-like multivalent cations: the correlations have been observed between the DNA–DNA distances in condensates and the length of polyamine chains used [15].

2. Basic equations

2.1. Model and approximations

We assume below that each toroidal cross-section is an *ideal hexagon* of closed DNA shells and the DNA turns are closed rings; see figure 1(C). The DNA curvature thus changes from one turn to another. The DNA wrapping in toroids is a special problem; below we show, however, that for realistic strengths of the DNA–DNA interactions the peculiarities of the model of DNA bending only slightly affect the results. Note that the local hexagonal symmetry can be distorted because of continuous circumference DNA wrapping: the crossovers between DNA turns can lead to 'topological defects' and hamper the toroidal growth [54]. However, we neglect this effect here.

Below, we consider only the DNA mechanical bending and neglect the loss of the DNA *entropy* upon confinement into the toroids (see [18]). The latter is a non-trivial problem [55]. For an ideal chain of N monomers of length a, the entropy of confinement into a sphere of radius K scales like $S_c \sim k_B N a^2 K^{-2}$. That is, for the confinement free energy F_c of a long semiflexible chain of length L into the sphere one can get $F_c \sim 2k_B T l_p L K^{-2}$ (for large K), that scales similarly to the average DNA bending energy, equation (8). Another estimate follows from the free energy loss of a worm-like chain confined in a tube of diameter D [56], $F_c \sim k_B T L l_p^{-1/3} D^{-2/3}$. This term would favour 'thicker' toroids in order to increase the polymer deflection length, $\lambda \sim l_p^{1/3} D^{2/3}$. In general, one can expect that thermal fluctuations disfavour the ideal DNA packing in toroids assumed below.

Although about 90% of DNA charge in toroids is expected to be neutralized by adsorbed cations [18, 57], the remaining 10% can in principle limit the deposition of a further DNA portion onto the toroids [18]. We expect however that DNA toroids as a whole (DNA + adsorbed and trapped cations) are *highly neutralized* due to the Donnan effect (accumulation of counterions in space between the DNA, with a high net negative potential); see [58]. We thus do not account for the effect of residual DNA charge on the toroid size. To get the value of the renormalized screening length inside the DNA toroids, we use the cylindrical cell model; see [26].

2.2. The Kornyshev–Leikin DNA–DNA interaction theory

We consider B-DNA as an ideal double helix with two thin continuous spirals of negative charges (DNA phosphates) and two spirals of positive charges in the middle between the phosphate spirals (cations adsorbed in the grooves); both are wrapped with a pitch of 34 Å on the surface of a rod with a low dielectric constant (DNA molecular core). Note that the treatment can be extended for discrete charges of phosphates and of cations [47] as well as for thermally smeared charge distribution on DNA [42].

The helix–helix electrostatic interaction is treated according to the *Kornyshev–Leikin theory* [39] (see this paper for derivations and for a detailed description of the model). DNA bent in toroids is expected to interact similarly to parallel helices in aggregates. The *pair* electrostatic interaction energy of two DNA at interaxial separation r in electrolyte solution can be approximated as the sum of zeroth (a_0) and first (a_1) and second (a_2) interaction harmonics [39, 41] (per ångström):

$$E_0(r) \approx a_0(r) - a_1(r) + a_2(r). \tag{1}$$

a_0 contains the repulsion of uniformly charged rods while the DNA helical symmetry enters $a_{1,2}$ [39, 40]; the dependence of $a_{0,1,2} > 0$ on the parameters of the model is presented

in [39, 40, 42]. The expressions for $a_{0,1,2}(r)$ are [39, 41]

$$a_0(r) = \frac{8\pi^2\sigma^2a^2}{\varepsilon}\left\{\frac{(1-\theta)^2K_0(\kappa r)}{[\kappa a K_1(\kappa a)]^2} - \sum_{l,m=-\infty}^{\infty}\frac{[f(l,\theta)K_{l-m}(\kappa_l r)]^2 I'_m(\kappa_l a)}{[\kappa_l a K'_l(\kappa_l a)]^2 K'_m(\kappa_l a)}\right\}, \tag{2}$$

$$a_{m=1,2}(r) = \frac{16\pi^2\sigma^2a^2[f(m,\theta)]^2K_0(\kappa_m r)}{\varepsilon[\kappa_m a K'_m(\kappa_m a)]^2}, \tag{3}$$

where $f(l,\theta) = f\theta + (-1)^l(1-f)\theta - \cos[0.4l\pi]$; $\kappa_l^2 = \kappa^2 + l^2(2\pi/H)^2$ are the effective reciprocal screening lengths for DNA–DNA interaction. Here $I_m(x)$ and $K_m(x)$ are the modified Bessel functions of the mth order, the prime denotes their derivatives; $\sigma \approx 16.8\,\mu$C cm^{-2} is the surface charge density of the B-DNA phosphates, $\theta > 0$ is the fraction of the phosphate charges neutralized by the adsorbed cations, $0 \leqslant f \leqslant 1$ and $(1-f)$ are the fraction of adsorbed cations in the minor and major DNA grooves, respectively; $\kappa = \sqrt{8\pi l_B n_0}$ is the reciprocal Debye screening length of the electrolyte solution, n_0 is the bulk concentration of simple salt; $a \approx 9$ Å is the radius of the B-DNA and $H \approx 34$ Å is its helical pitch; $\varepsilon \approx 80$ is the dielectric constant of the medium.

The $a_{1,2}$ are the dominant terms that differ the interaction between the double spirals (where the DNA–DNA interaction can be attractive, $E_0 < 0$) from that of uniformly charged rods (first term in curly brackets in equation (2)), which is always repulsive. Here, we neglect the 'frustration' term of the interaction energy [39, 42] (possible effects of higher harmonics are discussed in section 4) that should be valid for the separations relevant for DNA toroids, especially for highly compensated DNA (θ close to unity) and for adsorption of cations in the major groove (small f); see figure 3(b) in [42].

The strength of intermolecular interaction crucially depends on the patterns of adsorbed cations [40]. The DNA–DNA attraction becomes stronger with increasing the fraction of the DNA charge compensated by condensed cations, θ, and when more cations adsorb in the major DNA groove [40]; see figure 3. A typical value for DNA–DNA attraction strength is between -0.01 and $-0.05k_BT$ Å^{-1}, at DNA separations in toroids, $r \approx 28$ Å. This small energy value accumulates in toroids due to many DNA contacts with the neighbours and produces a giant interaction energy per toroid.

2.3. Energy

Smaller toroids with more DNA inside (with six neighbours) are favoured electrostatically, while the DNA bending energy favours larger toroids. As we show below, for a chosen DNA length L, there is a minimum of the total energy (electrostatic + bending) which corresponds to an optimal number of the DNA closed shells, the toroid generation n. Let $R = nr$ is the 'thickness' of DNA toroid and $3\sqrt{3}R^2/2$ is its cross-section; n is an integer; see figure 1(C). The concept of generations results in self-similar toroids for different L.

One can show, solving simple recurrent equations, that for a toroid of generation n the number of DNA turns is $3n^2+3n+1$ and the number of DNA–DNA interaction pairs is $9n^2+3n$. Thus, the average number of nearest neighbours is

$$\langle I(n)\rangle = 2(9n^2+3n)/(3n^2+3n+1). \tag{4}$$

This quantity is plotted in figure 2 together with an approximate expression for $\langle I\rangle$ obtained in [17] for not necessarily hexagonal toroidal cross-sections.

The DNA–DNA electrostatic interaction energy within the toroid of generation n can thus be written as the product of the pair interaction energy by the number of interaction pairs in the toroid,

$$E_{el}(n,K) = E_0(9n^2+3n)2\pi K. \tag{5}$$

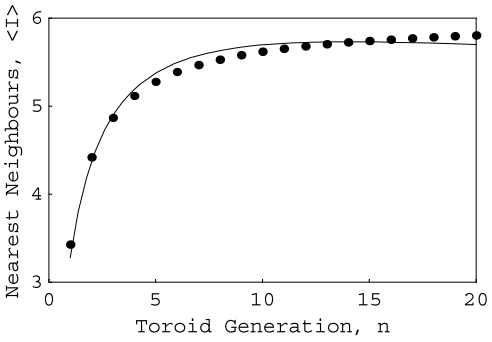

Figure 2. Average number of nearest neighbours in the DNA toroid of generation n. Dots: equation (4), solid curve: equation (10) in [18].

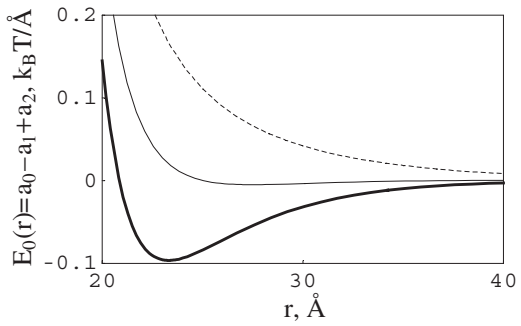

Figure 3. The pair B-DNA–B-DNA electrostatic interaction energy in solution as calculated from the Kornyshev–Leikin theory [39, 41, 42]. Juxtaposed DNA *double spirals* can attract each other if their phosphate charges are largely neutralized by the adsorbed cations and when the condensed cations reside in the major DNA groove. Parameters: $\kappa^{-1} = 7$ Å, (bold solid) $\theta = 0.9$, $f = 0.1$, (thin solid) $\theta = 0.8$, $f = 0.3$, and (dashed) $\theta = 0.5$, $f = 0.5$.

Here the *mean* radius of the toroid is K; see figure 1(A). We sum here only the nearest-neighbour DNA–DNA interactions since $a_{0,1,2}(r)$ decays nearly exponentially with r; see figure 2 in [42]. Also, the screening length inside a dense DNA lattice is considerably shorter than that in bulk solution due to the Donnan equilibrium [26, 42].

The energy of DNA mechanical bending E_b within such a toroid is obtained by summing the bending contributions of all the DNA turns with the corresponding radii, which gives

$$\frac{E_\mathrm{b}(n, K)}{k_\mathrm{B}T\pi l_\mathrm{p}} = \frac{2n+1}{K} + \sum_{m=1}^{n} \frac{2K(2n+1-m)}{K^2 - (mr\sqrt{3}/2)^2}. \tag{6}$$

The bending energy in the free DNA state is assumed to be zero. The bending energy grows when the toroids become smaller and the inner toroidal hole shrinks (the denominator in equation (6) is however never zero). The result of the minimization of the total energy

$$E(n, K) = E_\mathrm{el} + E_\mathrm{b} \tag{7}$$

with respect to n for a fixed DNA length $L = 2\pi K(3n^2 + 3n + 1)$ is presented in figure 4, for $l_\mathrm{p} = 500$ Å. This is the typical value for double-stranded B-DNA at physiological conditions [33]. The persistence length grows in low-concentration salt solutions; it reduces considerably upon binding of some multivalent cations to DNA [34] that facilitates the DNA toroidal condensation in solution of these cations.

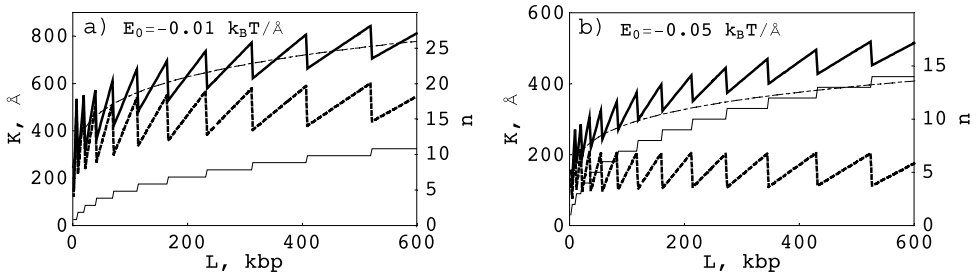

Figure 4. The mean radius of the DNA toroid K (bold), the radius of its inner hole (bold dotted), and toroid generation n (thin) versus the length of wrapped DNA L, plotted for two values of the DNA–DNA attraction strength. Dotted–dashed curves are obtained using $\langle E_b \rangle$.

The energy (6) is a more accurate expression than the *averaged* DNA bending energy within the toroid,

$$\langle E_b \rangle \approx k_B T l_p L/(2K^2). \tag{8}$$

That underestimates the bending energy and thus results in smaller toroids (dotted–dashed curves in figures 4, 5) than those obtained using equation (6), especially for small l_p. The minimization of $\langle E_b \rangle + E_{el}$ over n (or over K) at a fixed L results (for large n) in simple scaling relations for the toroidal dimensions

$$n \propto |E_0|^{1/5} L^{2/5} l_p^{-1/5} \qquad \text{and} \qquad K \propto |E_0|^{-2/5} L^{1/5} l_p^{2/5}; \tag{9}$$

see figure 5. Thus, since $E_{el}(n)$ distinguishes between the DNA on the surface of the toroid and in its inside, one can show that for the toroids the interaction energy scales like the 'surface tension', $E_{el} \propto |E_0| L^{1/2} K^{1/2}$ ($|E_0|$ plays the role of the surface tension modulus).

3. Results

The total energy of toroids for a fixed L has a minimum as a function of n; the energy value at the optimal n decreases with L. The mean toroid radius K reveals a tooth-like variation with increasing DNA length; see figure 4. The value of K increases on average because a continuous deposition of DNA on the toroid takes place when L grows. The typical radius of the toroid is $K \sim$ 300–800 Å, which is in the range of experimentally observed values. With increase of DNA–DNA attraction strength, E_0, the toroids become smaller in radius and larger in thickness (compare the 'thin' and 'fat' toroids in figure 4). For smaller l_p the toroids become smaller and their thickness grows; see figure 5(b).

There is a critical DNA length when the toroids start to be stable; this length decreases with increase of E_0: at $E_0 = -0.01 k_B T$ Å^{-1} a toroid with $n = 1$ is first formed for $L \sim 2$ kbp. For such interaction strength, the behaviour of the inner and outer toroidal radii is correlated. Also, per DNA turn, the bending energy ($\sim 3 k_B T$) is an order of magnitude smaller than the DNA–DNA interaction energy. Note that since for rod-like DNA condensates the rod length (thickness) is similar to the toroid circumference length (thickness) [18], one can expect that the DNA interaction and bending energy for toroids and rods are nearly the same.

At higher concentration of a simple salt—weaker DNA–DNA electrostatic interactions—we predict an increase of toroidal radius and a decrease in toroidal thickness; see figure 5(a). In this figure, we calculate E_0 explicitly according to equation (1); see [41, 42]. Here, we have also taken the Donnan equilibrium into account (here, the addition of salt changes only

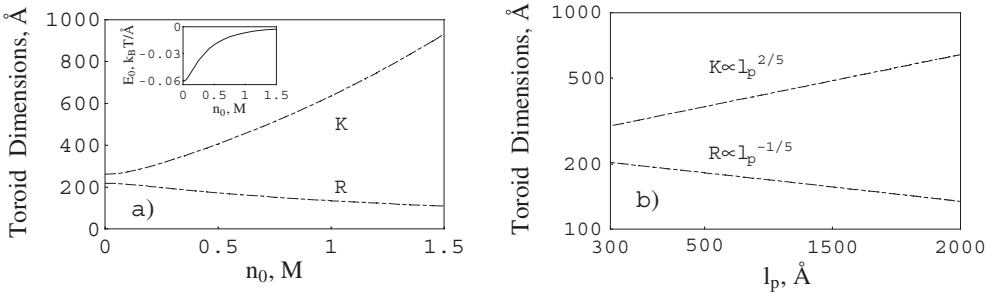

Figure 5. The mean radius of DNA toroids (K) and toroid 'thickness' (R), for different salt concentrations and DNA mechanical persistence lengths. The DNA–DNA interactions is calculated according to [41, 42], at conditions favouring the DNA–DNA attraction. The Donnan effect in DNA toroids is taken into account for the calculation of E_0 [42]; the inset shows the corresponding $E_0(n_0)$ dependence. Parameters: $\theta = 0.9$, $f = 0.1$, $L = 10^5$ bp, (a) $l_p = 500$ Å and (b) $n_0 = 0.4$ M (which corresponds to $E_0 = -0.026 k_B T$ Å^{-1}).

the screening length between the DNA in the toroids and does not affect the patterns of the adsorbed cations on DNA (θ and f are unchanged)).

The Kornyshev–Leikin theory [39] predicts that the adsorption of cations into the major groove strengthens the DNA–DNA attraction [40, 26]; see figure 3. Thus, it becomes clear why many multivalent cations, like spermidine and cohex, known to adsorb predominantly into the major groove, cause DNA condensation into toroids and in dense assemblies, whereas divalent and monovalent cations, which typically have a much weaker affinity to the major groove, do not condense DNA [40]. The difference in efficiency of cations of the same valence to condense DNA is likely to be due to the specificity of their interactions with the DNA and due to different effects on θ and f (different adsorption isotherms) that govern the intensity of DNA–DNA electrostatic interactions [40].

In principle, several interconnected toroids (a '*necklace*') can be formed of one DNA instead of a single toroid as is discussed above. However, comparing the energies for optimal toroidal dimensions in both cases, within this model a single toroid appears to be more favourable (some surface- or defect-specific energy terms can change this tendency).

The energy difference (per DNA turn) for a toroid of an optimal generation, and for a generation n close to this, decreases with increasing the toroidal thickness. That is, the probability distribution $P(n)$ calculated from this static model should become broader for 'fat' toroids. Note that one could allow the deposition of a single DNA turn, not a whole DNA shell, as an elementary act of toroid growth. Then, the cross-section would become non-ideally hexagonal and the $K(L)$ tooth-like dependence in figure 4 would be smoothened. We expect that closed outer DNA shells are the most stable states of the system; such 'islands of toroid stability' have also been reported in [53].

4. Discussion and outlook

4.1. DNA–DNA interactions

Above, we have used the interaction energy between *ideal* DNA duplexes [40] where DNA could attract each other because of the register of the phosphate strands and grooves on juxtaposed DNA. Real DNAs however are not ideal spirals. Non-ideality of the DNA structure, coming from the sequence-dependent variation of the twist angle between the nearest bp [59], hampers this strand–groove register. This has a profound effect on intermolecular interaction:

it appears that for long randomly sequenced torsionally rigid DNA the electrostatic attraction turns into repulsion [41]. The finite twist elasticity of the DNA backbone (the DNA twist elasticity modulus is $C \approx 3 \times 10^{-19}$ erg cm [60]) allows DNA to relax this twist sequence-dependent mismatch and to restore the strand–groove zipper-like register. This makes the DNA–DNA electrostatic interaction attractive again [42], although diminished as compared to that between the ideal duplexes [40].

Equation (1) is valid at large r when the mutual azimuthal twist angle $\delta\varphi$ between all DNA pairs on the lattice is zero [39], which ensures the existence of the 'electrostatic zipper'. At a smaller r, a more accurate expression is [39] $E_0 = a_0 - a_1 \cos\delta\varphi + a_2 \cos(2\delta\varphi)$. In this regime, the electrostatics can require a non-zero $\delta\varphi$ between two parallel DNA [39] and between DNA in the hexagonal lattice [42], i.e., the DNA lattice becomes '*frustrated*' [61, 42]; see figure 5(b) in [42]. Experiments also show that these frustrations appear in DNA columnar aggregates for $r \lesssim 35$ Å [62]. Similar DNA azimuthal frustrations can occur also in DNA toroids; the circumference wrapping of a single DNA may complicate the frustration picture (the defects/crossovers might be required for DNA packaging).

Note that the DNA wrapping in toroids may distort the electrostatic zipper attraction, even for ideal DNA. If all $\delta\varphi = 0$, the strand–groove register requires the length of each DNA turn to be divisible by the DNA helical pitch, H. In toroids, the DNA length varies continuously from one turn to another, i.e., a DNA twisting might be required within each DNA turn to restore an *integer* number of H per turn[3].

Note also that an effective attraction between DNA is necessary in toroids, while DNA packaging into viral capsids can be performed by motor proteins [64] and DNA–DNA attraction is not necessarily required. However, often the DNA in phages also adopts a hexagonal packing to optimize the entropic repulsion [6, 65].

4.2. Other models of toroid stability

Several models of the toroidal stability have been suggested in the literature. Bloomfield *et al* [18, 20] have investigated the formation of DNA toroids taking into account the residual DNA charge, rod-like electrostatic repulsion between the *DNA rods*, the entropic penalty for DNA compactification, and the bending and the mixing energy as well as the hydration forces which were the reason for the DNA collapse in their model. Odijk *et al* [51] have suggested a model for polymer- and salt-induced DNA toroidal condensation, where the DNA–DNA electrostatic interactions were also considered to be repulsive. Recently, Pereira *et al* [53] have studied the toroid stabilization in poor solvent and predicted a non-monotonic dependence of the toroidal radius on the DNA length. Closed DNA shells were shown to be favoured, minimizing unfavourable contacts with solvent; their model however neglects the DNA–DNA electrostatic interactions. The toroidal condensation of polymers (not of helical DNA!) has also been studied by computer simulations [66–68]. It was shown, in particular, that a semiflexible chain with short-range attractive interactions rolls into a toroid via a number of intermediate states; the loops appear usually from the chain ends and develop into toroids with time [66].

4.3. Outlook: kinetics of the toroid formation and nucleation

Bloomfield *et al* [18] have indicated that the size distribution of toroids is determined by *kinetic* rather than by thermodynamic factors. The first step for toroid formation is typically a closed DNA loop which serves as a nucleus for a further toroidal growth. In solution, one can expect

[3] One can speculate that in toroids the DNA keeps the mutual azimuthal angles predicted for a hexagonal lattice [42] over a long contact length, while a torsional kink-like adjustment occurs within a short segment along the DNA contact; see also [63].

the size of this loop to be of the order of the DNA persistence length, l_p, which is indeed close to a typical toroid radius.

The size distribution of toroids has been analysed by Hud *et al* [9] using kinetic arguments (the initial DNA loops are stabilized by attractive interactions along the DNA–DNA contacts). One can expect that for a short contact length this nucleus can dissociate, whereas for a longer contact length the only process is DNA deposition. Toroidal growth can occur inside and outside of the nucleus; toroidal growth with a constant DNA curvature radius was also suggested [9]. In [48] several mechanisms of DNA deposition on the toroids are analysed when no DNA threading through the inner toroid hole occurs (kinetically prohibited pathways); see also [69]. In general, the next DNA turn should have contacts with DNA on two or more preceding turns; see figure 1(C). This might cause some limitations on the local hexagonal packing and on the hexagonal toroidal cross-section; see figure 1(B). The toroid nucleation and growth depend on the amount of added salt [36] (if the toroid nucleation occurs more frequently the number of toroids will be smaller and their thickness larger, provided that there is a constant amount of free DNA in solution). Toroids also become smaller at elevated temperatures [30], which might be due to a smaller value of l_p.

5. Conclusions

The dimensions of DNA toroids has been estimated using the theory of electrostatic interactions between DNA duplexes [40, 42]. This theory treats correctly the DNA helical symmetry and gives rise to attractive DNA–DNA interactions. Within this theory, the specificity of DNA condensation by trivalent cations is naturally described in terms of helical patterns of DNA phosphates and of adsorbed cations on the DNA and a zipper-like electrostatic attraction of these patterns. In the presented model, the magnitude of DNA–DNA attractive forces governs the formation and determines the size of the DNA condensates (toroids and rods). Future experiments should reveal whether the tendencies predicted here for the toroidal size and thickness as a function of the DNA length, the DNA persistence length, the salt concentration and the DNA–DNA attraction strength are realistic, and how important the kinetic effects are.

Acknowledgments

We are grateful to Nicholas Hud for discussions, for permission to use the experimental figures and for providing a high-resolution version of them. Many comments of the referees are acknowledged.

References

[1] Finch J T, Lutter L C, Rhodes D, Brown R S, Rushton B, Levitt M and Klug A 1977 *Nature* **269** 29
[2] Richmond T J, Finch J T, Rushton B, Rhodes D and Klug A 1984 *Nature* **311** 532
[3] Luger K, Mäder A M, Richmond R K, Sangent D F and Richmond T J 1997 *Nature* **389** 251
[4] Reich Z, Watchel E J and Minsky A 1995 *J. Biol. Chem.* **270** 7045
[5] Englander J, Klein E, Brumfeld V, Sharma A K, Doherty A J and Minsky A 2004 *J. Bacteriol.* **186** 5973
[6] Cerritelli M E *et al* 1997 *Cell* **91** 271
[7] Olson N H *et al* 2001 *Virology* **279** 385
[8] Klimenko S M, Tikchonenko T I and Andreev V M 1967 *J. Mol. Biol.* **23** 523
[9] Hud N V, Downing K H and Balhorn R 1995 *Proc. Natl Acad. Sci. USA* **92** 3581
[10] Hud N V, Allen M J, Downing K H, Lee J and Balhorn R 1993 *Biochem. Biophys. Res. Commun.* **193** 1347
[11] Allen M J, Bradbury E M and Balhorn R 1997 *Nucleic Acids Res.* **25** 2221
[12] Gosule L C and Schellman J A 1976 *Nature* **259** 333
[13] Laemmli U K 1975 *Proc. Natl Acad. Sci. USA* **72** 4288

[14] Widom J and Baldwin R L 1980 *J. Mol. Biol.* **144** 431
[15] Schellman J A and Parthasarathy N 1984 *J. Mol. Biol.* **175** 313
[16] Wilson R W and Bloomfield V A 1979 *Biochemistry* **18** 2192
[17] Arscott P G, Li A-Z and Bloomfield V A 1990 *Biopolymers* **30** 619
[18] Bloomfield V A 1991 *Biopolymers* **31** 1471
[19] Bloomfield V A 1996 *Curr. Opin. Struct. Biol.* **6** 334
[20] Bloomfield V A 1997 *Biopolymers* **44** 269 and references therein
He S, Arscott P G and Bloomfield V A 2000 *Biopolymers* **53** 329
[21] Marx K A and Ruben G C 1983 *Nucleic Acids Res.* **11** 1839
[22] Marx K A and Ruben G C 1986 *J. Biomol. Struct. Dyn.* **4** 23
[23] Golan R *et al* 1999 *Biochemistry* **38** 14069
[24] Hsiang M W and Cole R D 1977 *Proc. Natl Acad. Sci. USA* **72** 4288
[25] Leikin S, Rau D C and Parsegian V A 1991 *Phys. Rev.* A **44** 5272
[26] Cherstvy A G, Kornyshev A A and Leikin S 2002 *J. Phys. Chem.* B **106** 13362
[27] Ma C and Bloomfield V A 1994 *Biophys. J.* **67** 1678
[28] Hultgren A and Rau D C 2004 *Biochemistry* **43** 8272
[29] Yevdokimov Yu M, Skuridin S G and Salyanov V I 1988 *Liq. Cryst.* **3** 1443
[30] Conwell C C and Hud N V 2004 *Biochemistry* **43** 5380
[31] Grosberg A Yu and Zhestkov A V 1986 *J. Biomol. Struct. Dyn.* **3** 859
Vasilevskaya V V, Khokhlov A R, Kidoaki S and Yoshikawa K 1997 *Biopolymers* **41** 51
[32] Fang Y and Hoh J H 1998 *Nucleic Acids Res.* **26** 588
[33] Baumann C G, Smith S B, Bloomfield V A and Bustamante C 1997 *Proc. Natl Acad. Sci. USA* **94** 6185
[34] Williams L D and Maher L J III 2000 *Annu. Rev. Biophys. Biomol. Struct.* **29** 497
[35] Shen M R, Downing K H, Balhorn R and Hud N V 2000 *J. Am. Chem. Soc.* **122** 4833
[36] Conwell C C, Vilfan I D and Hud N V 2003 *Proc. Natl Acad. Sci. USA* **100** 9296
[37] Hansma H G *et al* 1998 *Nucleic Acids Res.* **26** 2481
[38] Leikin S, Rand R P, Rau D C and Parsegian V A 1993 *Annu. Rev. Phys. Chem.* **44** 369
[39] Kornyshev A A and Leikin S 1997 *J. Chem. Phys.* **107** 3656
Kornyshev A A and Leikin S 1998 *J. Chem. Phys.* **108** 7035 (erratum)
[40] Kornyshev A A and Leikin S 1999 *Phys. Rev. Lett.* **82** 4138
[41] Kornyshev A A and Leikin S 2001 *Phys. Rev. Lett.* **86** 3666
[42] Cherstvy A G, Kornyshev A A and Leikin S 2004 *J. Phys. Chem.* B **108** 6508
[43] Oosawa F 1971 *Polyelectrolytes* (New York: Dekker)
[44] Rouzina I and Bloomfield V A 1996 *J. Phys. Chem.* **100** 9977
Grønbech-Jensen N, Mashl R J, Bruinsma R F and Gelbart W M 1997 *Phys. Rev. Lett.* **78** 2477
Ha B-Y and Liu A J 1997 *Phys. Rev. Lett.* **79** 1289
Podgornik R and Parsegian V A 1998 *Phys. Rev. Lett.* **80** 1560
Golestanian R and Liverpool T B 2002 *Phys. Rev.* E **66** 051802
[45] Korolev N, Lyubartsev A P, Rupprecht A and Nordenskiold L 1999 *Biophys. J.* **77** 2736
Korolev N, Lyubartsev A P, Rupprecht A and Nordenskiold L 2001 *Biopolymers* **58** 268
[46] Allahyarov E, Gompper G and Löwen H 2004 *Phys. Rev.* E **69** 041904 and references therein
[47] Kornyshev A A and Leikin S 1998 *Proc. Natl Acad. Sci. USA* **95** 13579
[48] Hud N V and Downing K N 2001 *Proc. Natl Acad. Sci. USA* **98** 14925
[49] Lepault J *et al* 1987 *EMBO J.* **6** 1507
[50] Rau D C and Parsegian V A 1992 *Biophys. J.* **61** 260
[51] Ubbink J and Odijk T 1995 *Biophys. J.* **68** 54
[52] Odijk T 1998 *Biophys. J.* **75** 1223
[53] Pereira G G and Williams D R M 2000 *Europhys. Lett.* **50** 559
[54] Park S Y, Harries D and Gelbart W M 1998 *Biophys. J.* **75** 714
[55] Mondescu R P and Muthukumar M 1998 *Phys. Rev.* E **57** 4411
[56] Odijk T 1983 *Macromolecules* **16** 1340
[57] Bloomfield V A, Wilson R W and Rau D C 1980 *Biophys. Chem.* **11** 339
[58] Cherstvy A G *et al* 2005 *Sensors Actuators* A at press
[59] Kabsch W, Sander C and Trifonov E N 1982 *Nucleic Acids Res.* **10** 1097
Gorin A A, Zhurkin V B and Olson W K 1995 *J. Mol. Biol.* **247** 34
Olson W K, Gorin A A, Lu X-J, Hock L M and Zhurkin V B 1998 *Proc. Natl Acad. Sci. USA* **95** 11163
[60] Horowitz D S and Wang J C 1984 *J. Mol. Biol.* **173** 75
Frank-Kamenetskii M D *et al* 1985 *J. Biomol. Struct. Dyn.* **2** 1005

[61] Harreis H M, Kornyshev A A, Likos C N, Löwen H and Sutmann G 2002 *Phys. Rev. Lett.* **89** 018303
[62] Strey H H, Wang J, Podgornik R, Rupprecht A, Yu L, Parsegian V A and Sirota E B 2000 *Phys. Rev. Lett.* **84** 3105
[63] Kornyshev A A and Wynveen A 2004 *Phys. Rev.* E **69** 041905
[64] Kindt J, Tzlil S, Ben-Shaul A and Gelbart W M 2001 *Proc. Natl Acad. Sci. USA* **98** 13671
[65] Purohit P K, Kondev J and Phillips R 2003 *Proc. Natl Acad. Sci. USA* **100** 3173
[66] Schnurr B, MacKintosh F C and Williams D R M 2000 *Europhys. Lett.* **51** 279
[67] Noguchi H and Yoshikawa K 2000 *J. Chem. Phys.* **113** 854
Noguchi H and Yoshikawa K 1998 *J. Chem. Phys.* **109** 5070
[68] Stevens M 2001 *Biophys. J.* **80** 130
[69] Kulić I M, Andrienko D and Deserno M 2004 *Europhys. Lett.* **67** 418